Atherosclerosis 290 (2019) 19–30

Contents lists available at ScienceDirect

Atherosclerosis

journal homepage: www.elsevier.com/locate/atherosclerosis

Lysophosphatidic acid decreased macrophage foam cell migration correlated with downregulation of fucosyltransferase 8 via HNF1α

Linmu Chen[a], Jun Zhang[a], Xi Yang[a,b], Yan Liu[a], Xiao Deng[a], Chao Yu[c,*]

[a] Institute of Life Science, Chongqing Medical University, Chongqing, 400016, PR China
[b] College of Basic Medicine, Inner Mongolia Medical University, Hohhot, 010110, China
[c] College of Pharmacy, Chongqing Medical University, Chongqing, 400016, PR China

HIGHLIGHTS

- Macrophage-derived foam cells induced by LPA have a diminished capacity of migration.
- Downregulation of Fut8 and α-1, 6-fucosylation levels is involved in the decreased mobility of foam cells.
- LPA can reduce the combination between HNF1α and Fut8 promoter region by activating its $LPA_{1,\ 3}$ receptors.

ARTICLE INFO

Keywords:
LPA
Foam cell migration
Fucosyltransferase 8
$LPA_{1,\ 3}$ receptors
HNF1α

ABSTRACT

Background and aims: Aberrant fucosylation, such as α-1,6 fucosylation catalyzed by fucosyltransferase 8 (Fut8), is associated with reduced cell migration and is responsible for cholesterol-enriched foam cell accumulation in the intima in the early stage of atherosclerosis.

The current study evaluated the impact of glycosyltransferases on foam cell migration induced by lysophosphatidic acid (LPA) and its potential mechanism.

Methods: The mobility of foam cells was evaluated via transwell and scratch assays. The expression of Fut8 and α-1,6 fucosylation of proteins were assessed by RT-PCR, Western blotting, etc. Overexpression of Fut8 was used to explore the direct relationship between Fut8 and foam cell migration. Dual luciferase reporter assay was performed to determine whether the regulation of Fut8 by LPA occurred at the transcriptional level. Binding of hepatocyte nuclear factor 1-alpha (HNF1α) to the Fut8 promoter was assessed by electrophoretic mobility shift assay and chromatin immunoprecipitation assay.

Results: We found that the migration capacity of foam cells induced by LPA was significantly decreased. Fut8 and α-1,6 fucosylation showed the most obvious decline after treatment with 200 μM LPA for 24 h. Overexpression of Fut8 was able to restore the foam cell migration capacity. Another important finding was that the LPA_1 and LPA_3 ($LPA_{1,3}$) receptors were involved in the regulation of Fut8. It is interesting to note that LPA led to a decrease in Fut8 gene transcription activity, and HNF1α transcription factor played a positive role in downregulation of Fut8 promoter activity.

Conclusions: Our results strongly indicated that the LPA-$LPA_{1,\ 3}$ receptor-HNF1α pathway is involved in the downregulation of Fut8, leading to diminished foam cell migration.

1. Introduction

Atherosclerosis (AS) is a disease of the medium- and large-sized arteries and is characterized by lipid accumulation in the arterial wall [1]. Focal retention of macrophage foam cells in the subendothelial space is a hallmark of atherosclerotic lesions [2]. Unlike in other tissues, macrophage foam cells appear to have a diminished capacity to migrate in atherosclerotic plaques [3]. Impaired egress is expected to compound macrophage accumulation within plaques, thus contributing to the build-up of necrotic pools [4]. Restoration of the capacity of monocyte-derived cells to leave plaques is expected to facilitate regression. By tracing the migratory behavior of human monocytes, Llodra et al. thought that progression of atherosclerotic plaques might result not only from robust monocyte recruitment into the arterial walls but also from reduced migration of these cells from lesions [5]. Using a model of atherosclerosis regression, Feig et al. found that macrophage

* Corresponding author. College of Pharmacy, Chongqing Medical University, No. 1 Yixueyuan Road, Yuzhong District, Chongqing, 400016, PR China.
E-mail address: yuchaom@163.com (C. Yu).

https://doi.org/10.1016/j.atherosclerosis.2019.09.001
Received 9 May 2019; Received in revised form 19 August 2019; Accepted 10 September 2019
Available online 11 September 2019
0021-9150/

(CD68 $^{+}$ cell) migration and induction of the C–C chemokine receptor type 7 (CCR7) were associated with decreased plaque content after HDL-C normalization [6]. If the mechanisms of diminished migration were elucidated, therapies designed to reinforce events that promote macrophage foam cell removal could likely improve clinical success in reducing further critical cardiovascular events.

Glycosylation is a general protein post-translational modification that occurs in the endoplasmic reticulum (ER) and Golgi apparatus [7]. More than half of all proteins are glycosylated, and thus this process plays an important role in normal physiological processes, including protein folding, stability, and secretion [8]. As mentioned in the literature, post-translational glycosylation by glycosyltransferases is necessary for progression and regression of atherosclerosis. Compared with control *ApoE*$^{-/-}$ mice, beta-galactoside alpha-2,3-sialyltransferase IV$^{-/-}$ (*ST3Gal-IV*$^{-/-}$) *ApoE*$^{-/-}$ mice displayed minor atherosclerotic plaque sizes and minimal inflammatory cell content [9]. In the early stage of atherosclerosis, our previous work found that degradation of beta-galactoside alpha-2,6 sialyltransferase I (ST6Gal-I) downregulated α-2, 6 sialylation of VE-cadherin, resulting in the impairment of endothelial tight junctions and promoting monocyte-endothelial cell adhesion [10]. Our further experiments showed that decrease in sialylation of β-catenin in the endothelium modified by ST6Gal-I was responsible for diminished monocyte transendothelial migration [11]. However, the relationship between glycosyltransferases and diminished macrophage foam cell migration remains unknown.

In the past decades, many efforts were put forth to assess the biological functions of protein α-1, 6 fucosylation, especially in tumor migration and invasion. Wang et al. found that overexpression of Fut8 increased androgen-independent PCa (PC3) cell migration, and loss of Fut8 decreased cell motility in androgen-dependent PCa (LNCaP) cells [12]. By affecting the core fucosylation level of E-cadherin, overexpression of Fut8 inhibited giant lung carcinoma 95C cell migration, whereas knockdown of Fut8 enhanced migration of giant lung carcinoma 95D cells [13]. Upregulation of Fut8 only inhibited the proliferation of cells from gastric cancer cell lines BGC-823 and SGC-7901 but with no significant influence on migration [14]. As such, Fut8 was reported to play a role in the progression of tumor cell migration, but the correlations were controversial.

In thus study, we induced macrophage foam cell formation with 200 μM LPA treatment for 24 h [15]. We sought to address the question of the relationship between Fut8 and foam cell migration and how Fut8 was influenced in atherosclerosis. The answer could provide new insights into the promotion of migration of foam cells from atherosclerosis plaques.

2. Materials and methods

2.1. Cell culture and reagents

Murine RAW 264.7 and human HEK293T cell lines were obtained from the American Type Culture Collection (ATCC, Manassas, US). The cells were cultured in DMEM supplemented with 10% FBS (BI, Israel), under a humidified atmosphere at 37 °C and 5% CO_2. Fluorescein or biotin-labeled Sambucus nigra lectin (SNA, α-2, 6 sialylation), Maackia amurensis lectin I (MALI, α-2, 3 sialylation) and Aleuria aurantia lectin (AAL, total fucosylation) were purchased from Vector Laboratories (Peterborough, UK). Goat Fut8 and Fut7 polyclonal antibodies were purchased from Santa (Dallas, TX, USA). Rabbit HNF1α, HNF4α and Fut8 monoclonal antibodies were purchased from Abcam (Oxford, UK). Rabbit LPA_1, LPA_3 and β-actin polyclonal antibodies were purchased from Bioss (Beijing, China). Cycloheximide (CHX), actinomycin D (AMD) and thioglycolate medium were purchased from Sigma (St. Louis, MO, USA).

2.2. Migration assay

The scratch assay was performed according to a previous study, with some modifications [16]. In brief, cells were treated with 200 μM LPA for 24 h, and 200 μl pipette tips were used to scratch the cell layers. Subsequently, the wounds were washed gently with PBS and further cultured in serum-free medium for 24 h. Cells were imaged under an inverted microscope (Olympus Corporation, Tokyo, Japan).

The transwell assay was performed according to the previous study with some modifications [16]. RAW 264.7 cells were placed in the upper chamber, and 200 μM LPA was added. After 24 h, the medium in the upper chamber was removed, and serum-free medium was added. The lower chamber was filled with medium containing 10% FBS as a chemotaxis force. After 24 h, cells on the upper chamber were removed with cotton swabs, and cells on the underside were fixed with 4% PFA for 10 min at room temperature (RT). The cells were stained with 0.1% crystal violet (Solarbio, Beijing, China) for 10 min, and migrating cells were monitored under a light microscope (Olympus Corporation, Tokyo, Japan).

2.3. Western blot

Western blot was performed as previously described [10]. In brief, cell lysates were centrifuged at 12,000 rpm for 15 min at 4 °C. Concentrations of protein samples were determined with BCA protein assay kit. The proteins were separated by 6–10% sodium dodecyl sulfate-polyacrylamide gel electrophoresis and transferred to a polyvinylidenedifluoride membrane. The blots were incubated overnight with antibodies. The blots were washed three times (10 min each) in Tris-Buffered Saline Tween-20 (TBST), followed by 60 min incubation with the appropriate horseradish peroxidase-conjugated secondary antibody. The specific proteins were visualized using an Enhanced Chemiluminescence kit (KeyGEN BioTECH, Jiangsu, China).

2.4. Real-time PCR

Total cellular RNA was extracted from the cells using an Ultrapure RNA Kit (CWbio, Beijing, China). The total RNA (1 μg) was subjected to an RT reaction with the PrimeScriptTM RT reagent kit (Takara, Dalian, China). Real-time PCR was performed using an iCycleriQ real-time detection system with SYBR Premix Ex TaqTM II. The targeted genes were amplified with the following primers: Fut1 Forward: 5′ CATGTG CGTCGTGGAGACTA 3’; Fut1 Reverse: 5′ CAGCGAAGACCACATCACCA 3’; Fut2 Forward: 5′ ATCCACCTCCAGCAACGAAT 3’; Fut2 Reverse: 5′ CTGGCTGTGTCG- CTGTGTAA 3’; Fut4 Forward: 5′CGAATCGCCCTCC CATACTC 3’; Fut4 Reverse: 5′ GCTGGTGGTAGTAACGGACC 3’; Fut7 Forward: 5′ CAAA CCCGGCAATCTCTCC- T 3’; Fut7 Reverse: 5′ AGTT GAAGATGCCCCGGAAG 3’; Fut8 Forward: 5′ CTGGT- TCCTGGCGTTG GATT 3’; Fut8 Reverse: 5′CTCAGCCATTCGCC TCAAGT 3’; HNF1α Forward: 5′ GCACCAGAGACCCACGTGCC 3’; HNF1α Reverse: 5′ GGCTT- CCCCTCAGCTCCCGA 3’; β-Actin Forward: 5′ AAGACCTCTAT GCCAACAC3’; β-Actin Reverse: 5′ CTGCTTGCTGATCCACAT 3’.

2.5. Isolation of mouse peritoneal macrophages

Male C57BL/6J mice (8 weeks old) were purchased from the Animal Experimental Center of Chongqing Medical University (Chongqing, China). The procedure was conducted as previously described. In brief, mice were intraperitoneally injected with 1 mL 3% thioglycollate medium. After 7 days, the mice were euthanized, and 10 mL sterile cold PBS was injected into the abdominal cavity to wash out the macrophages. The cells were counted after resuspension in culture medium and seeded in 24-well plates or 6-well plates for further experiments.

2.6. Animal model of atherosclerosis

Male $ApoE^{-/-}$ mice (C57BL/6J, 6 weeks old; n = 22) were purchased from HFK Bioscience Co., Ltd. (Beijing, China). The mice were housed in cages (temperature, 22 °C) with a 12-h light/dark cycle and allowed ad libitum access to food and water. $ApoE^{-/-}$ mice were randomly divided into three groups: baseline group (n = 6), control group (n = 8) and rosuvastatin group (n = 8). To establish the atherosclerosis animal model, all $ApoE^{-/-}$ mice were maintained on a Western diet containing 0.15% cholesterol and 21% fat (MD12015, Medscience Ltd, Jiangsu, China) for 12 weeks. The mice in the baseline group were sacrificed. The other two groups were fed the Western diet for the next four weeks. In the meantime, mice in the rosuvastatin group and control group were administered rosuvastatin (10 mg/kg/day, diluted in saline, Abmole, USA) or saline every day by gavage, respectively. After centrifugation to obtain serum, serum lipid (TC, total cholesterol; TG, triglyceride; LDL-C, low-density lipoprotein cholesterol; HDL-C, high-density lipoprotein cholesterol) levels were analyzed by an automatic analyzer (Mindray BS-220, Shenzhen, China). The thoracic aorta was obtained by thoracotomy and fixed in 4% PFA for further analyses. After dehydration using graded saccharose, a portion of the heart containing the aortic root was placed in an optimal cutting temperature compound (OCT) embedding medium and quickly frozen. OCT-embedded tissue was mounted in a Leica RM2145 cryostat, and 8 μm cross-sections were collected. A cryosection from each mouse was stained with Oil-Red O and H&E. Images were obtained under a light microscope (Olympus Corporation, Tokyo, Japan). This study was performed in accordance with the recommendations of the Chongqing Management Approach for Laboratory Animals (Chongqing Government Order No.195). The protocol was approved by the Institutional Review Board of Chongqing Medical University.

2.7. Plasmid and overexpression

Fut8 overexpression plasmid was generated by subcloning PCR-amplified full-length mouse Fut8 cDNA into the pCDNA3.1 vector. HNF1α overexpression plasmid (pReceiver-M29 expression clone) was purchased from FulenGen (Guangzhou, China). Plasmid transient transfection was performed as previously described. After transfection, LPA was added for 24 h, and further experiments were performed.

2.8. Dual-luciferase assay

The pGL3-basic vector-based reporter gene containing the mouse Fut8 promoter region −2102/-7 was constructed. The plasmid was transiently transfected into HEK293T cells in the presence of LPA or not. After 48 h, the cells were harvested and lysed. The luciferase activity was measured using the dual-luciferase reporter assay system (Promega, Madison, US), and Renilla luciferase was used for normalization. A series of truncated Fut8 promoter luciferase reporter vectors were constructed and identified and were transfected into HEK293T cells to observe the possible regions showing relationships with the transcription factor.

2.9. Electrophoretic mobility shift assay (EMSA)

The nuclear extracts were prepared from control and LPA-treated cells, according to the manufacturer's instruction (P0027, Beyotime, Shanghai, China), and BCA was used to quantify protein. Biotin 5′ end-labeled DNA targets were obtained from Tsingke Co., Ltd. (Chengdu, China). The sequences are listed as follows: Forward 5′ GAAGAAGAG TTAATGGTACTTA 3’; and Reverse 5′ TAAGTACCATTAACTCTTCTTC 3’. A native 6% polyacrylamide gel was pre-electrophoresed in 0.5X TBE for approximately 60 min. According to the manufacturer's instructions, 10X binding buffer, 50% glycerol, and $MgCl_2$ were added to the mixture. The electrophoresis was performed at 100 V for 45–60 min, followed by transfer at 100 V for 45 min and crosslinking of the DNA fragments and protein with UV light for 20 min. The proteins were visualized using a Chemiluminescent Nucleic Acid Detection Module kit (Invitrogen, Shanghai, China).

2.10. Chromatin immunoprecipitation (ChIP)

In brief, RAW 264.7 cells were fixed with 37% formaldehyde (final concentration, 1%) and lysed in buffer A and B (supplemented with protease inhibitors) using a micrococcal nuclease to isolate the nuclei. The nuclei were resuspended in 1X ChIP buffer (supplemented with protease inhibitors) and sonicated to shear genomic DNA to an average fragment length of 150–900 bp. Lysates were centrifuged, and the supernatants were collected. Fifty microliters of each sample were used as the input control. The supernatants underwent overnight immunoprecipitation (with IgG or HNF1α), elution, reverse cross-linking and protease K digestion according to the manufacturer's protocol (SimpleChip™ Enzymatic Chromatin IP Kit, CST, US). Purified DNA extracts were analyzed by RT-PCR using the primer pairs that cover the predicted HNF1α binding elements in the Fut8 promoter region. The primers are listed as follows: forward: 5′ GAAGGGATATGAGGGTTTG TAG 3’; and reverse: 5′ TAGTCCACCCTAAACC-TGGAAT 3’.

2.11. Statistical analysis

The data are presented as mean ± SD. When three or more groups existed, one-way ANOVA with Tukey's *post hoc* test or a two-way ANOVA with Bonferroni's *post hoc* test was applied. When only two groups existed, Student's *t*-test was applied. A value of $p < 0.05$ was considered statistically significant.

3. Results

3.1. Total protein fucosylation was decreased in the procedure of inhibiting migration of foam cells

Our previous work demonstrated that 200 μM LPA, which simulated high concentrations under pathological conditions [17,18], directly induced macrophage-derived foam cell formation [15]. The migration of foam cells was evaluated by scratch assay and transwell assay. As shown in Fig. 1A, closure of the wound gap in the scratch assay was delayed in the LPA-treated group compared with the control group. Consistently, the transwell assay revealed that the number of migrated cells per field in the LPA-treated group was less than that in the control group (Fig. 1B). Therefore, we concluded that foam cells induced by LPA had a diminished capacity to migrate. Post-translational glycosylation by glycosyltransferases is important for the progression of atherosclerosis [19]. To assess the changes of glycosylation in foam cells, we used flow cytometry and lectin blots to detect the total protein α-2, 6 sialylation, α-2, 3 sialylation and total fucosylation levels with specific fluorescein or biotin-labeled lectins [20].The total protein α-2, 6 sialylation and α-2, 3 sialylation levels were not significantly altered after LPA treatment, according to flow cytometry (Fig. 1C). We observed a decrease in expression of SNA and MAL I in the lectin-blot assay (Fig. 1D and E). The flow cytometry results showed that the fluorescence intensity of AAL showed a decreasing trend after LPA treatment (Fig. 1F). Additionally, we observed similar results from the AAL-lectin blot (Fig. 1G). To confirm the universality of the experimental results, murine peritoneal macrophages were isolated. The scratch assay revealed that LPA led to slower closure of the wound gap (Supplementary Fig. 1A), and the transwell assay showed that fewer cells migrated to the lower chamber in the LPA-treated group (Supplementary Fig. 1B). Together, these results demonstrated that total protein fucosylation levels were notably decreased after LPA treatment.

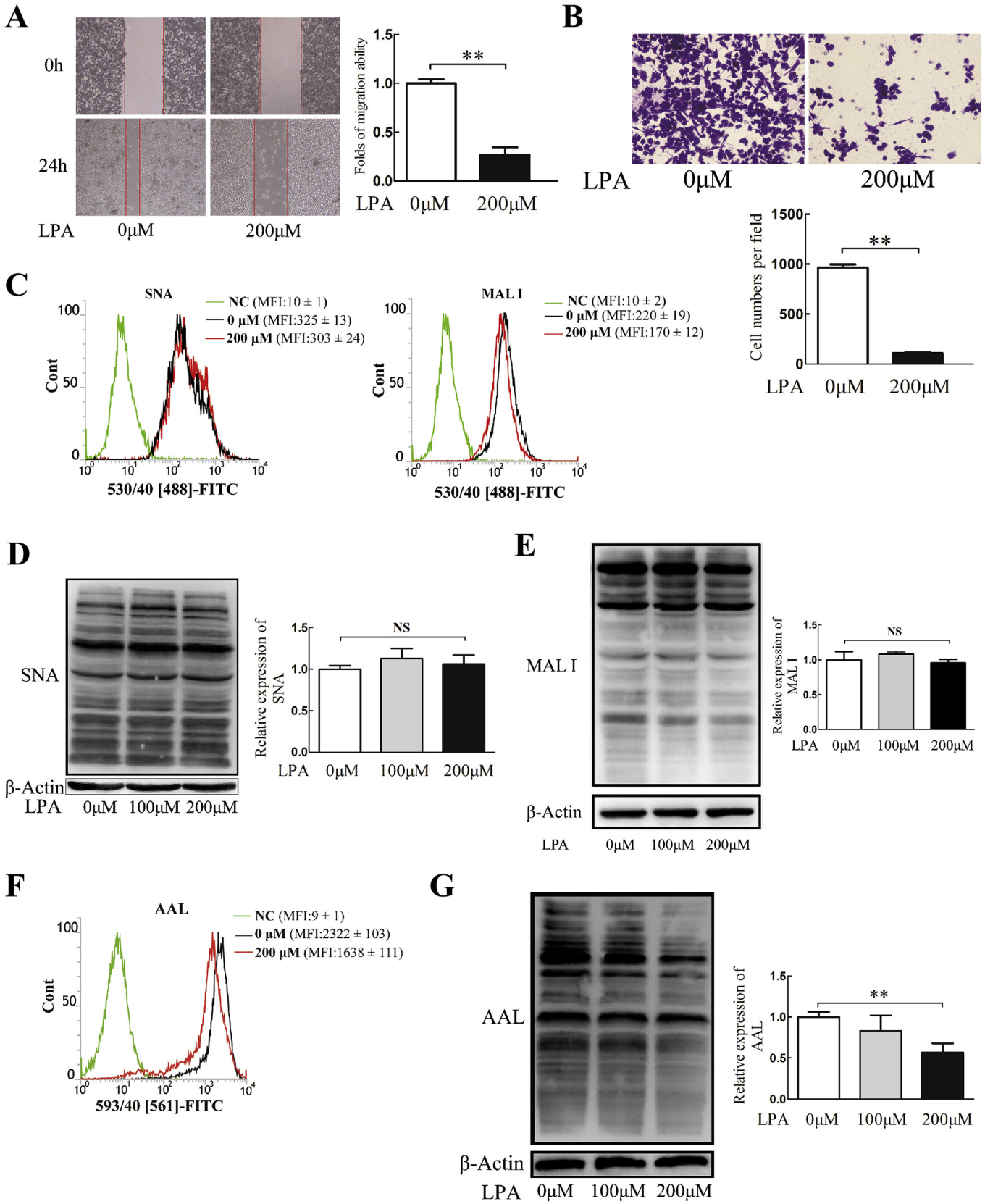

Fig. 1. Glycosylation changes in the formation of foam cell induced by LPA.
(A) Migration of foam cells derived from RAW 264.7 cells examined by scratch assay (40X magnification). (B) Migration of foam cells derived from RAW 264.7 cells examined by transwell assay (400X magnification). (C) Expression of α-2, 6 sialylation and α-2, 3 sialylation determined by flow cytometry assay. (D and E) Lectin blotting assays conducted to characterize the levels of total protein α-2, 6 sialylation and α-2, 3 sialylation in RAW 264.7 cells. (F) Expression of total fucosylation determined by flow cytometry assay. (G) Lectin blot assays conducted to characterize the levels of total protein fucosylation in RAW 264.7 cells. *$p <$ 0.05. LPA, lysophosphatidic acid; SNA, sambucus nigra lectin; NC, negative control; MAL I, maackia amurensis lectin I; AAL, aleuria aurantia lectin; NS, not significant.

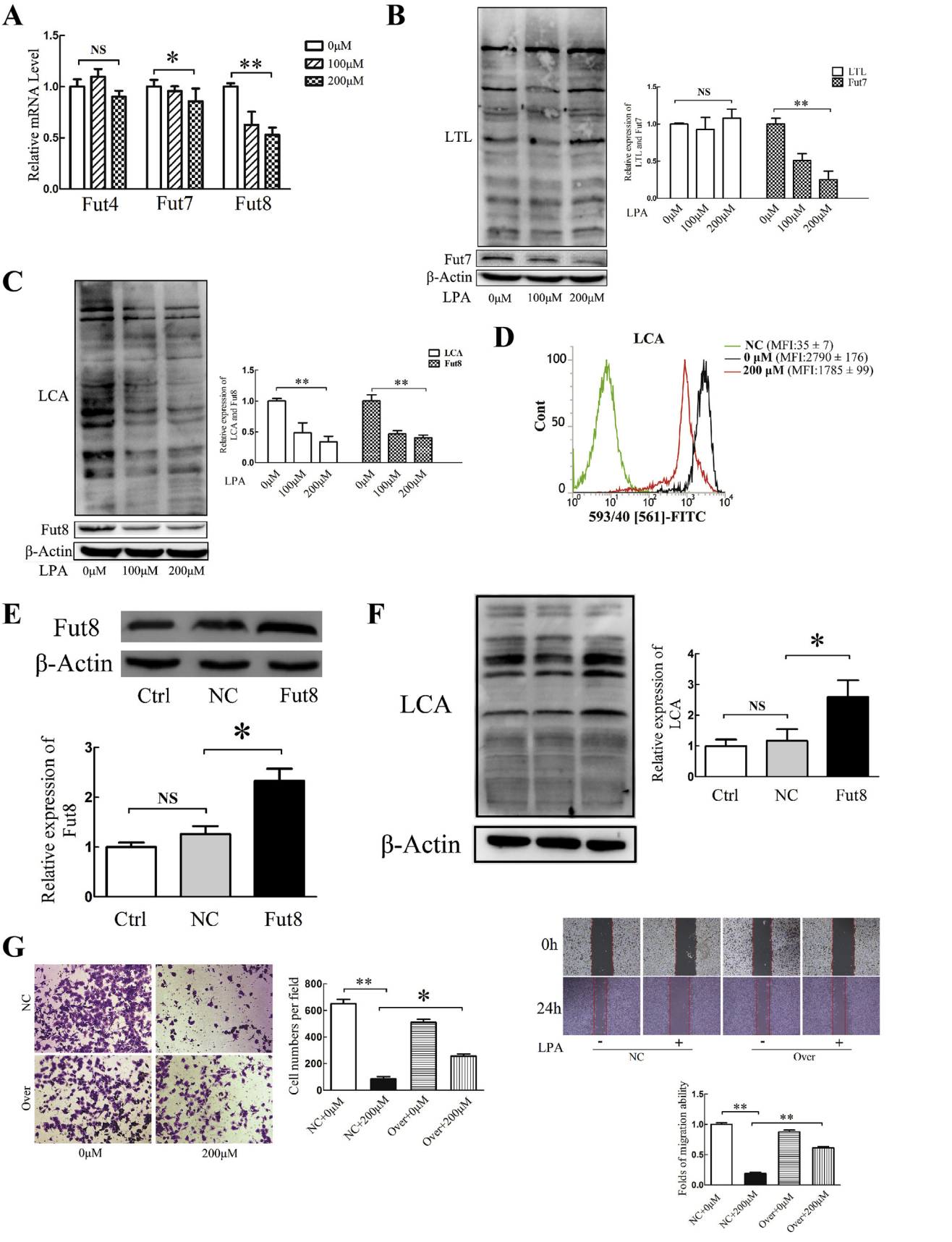

(caption on next page)

Fig. 2. Fut8 levels had the most significant change in formation of foam cells.
(A) Changes in fucosyltransferase mRNA expression levels detected by RT-PCR. (B) Western blot and lectin blot assays to characterize the levels of Fut7, protein α-1, 3/4 fucosylation in RAW 264.7 cells. (C) Western blot and lectin blot assays to characterize the levels of Fut8 and protein α-1, 6 fucosylation in RAW 264.7 cells. (D) Flow cytometry assay to characterize the levels of protein α-1, 6 fucosylation in RAW 264.7 cells. (E) Overexpression of Fut8 detected by Western blot. (F and G) Pretreatment with pCDNA3.1-Fut8 plasmid for 24 h, 200 μM LPA for 24 h was used to induce foam cell formation. Migration of foam cells derived from RAW 264.7 was examined by transwell (400X magnification) and scratch assays (40X magnification). $^{*}p < 0.05$; $^{**}p < 0.01$. LPA, lysophosphatidic acid; LTL, lotus tetragonolobus lectin; LCA, lens culinaris lectin; NC, negative control; Crtl, control; Over, overexpression; NS, not significant.

3.2. Expression of Fut8 was correlated with the migration of foam cells

Fucosylated glycan can be divided into three types in mice: α-1, 2 fucosylation (Fut1 and Fut2), α-1, 3/4 fucosylation (Fut4 and Fut7) and α-1, 6 fucosylation (Fut8) [21]. RT-PCR was used to assess the changes of fucosyltransferases. As shown in Fig. 2A, we found that the mRNA levels of Fut7 and Fut8 were significant decreased in the LPA-treatment group, whereas Fut4 showed no change, and other fucosyltransferases were not detected. We observed a decrease in Fut7 protein levels. However, α-1, 3/4 fucosylation levels showed no obvious changes in lectin-blot analysis (Fig. 2B). As indicated in Fig. 2C and D, LPA clearly decreased Fut8 protein level and α-1, 6 fucosylation level in the lectin-blot and flow cytometry assay. Similarly, the protein and mRNA levels of Fut8 were decreased in foam cells induced by peritoneal macrophages (Supplementary Figs. 2A and B). To definitely confirm the important function of Fut8 in cell migration, we used a pCDNA3.1-Fut8 plasmid to overexpress Fut8 in RAW 264.7 cells. The results of WB confirmed the validity of overexpression (Fig. 2E). After pretreatment with pCDNA3.1-Fut8 plasmid, we found that the numbers of migrated cells on the underside were much greater than those in the LPA group in the transwell assay (Fig. 2F). Closure of the wound gap was faster after restoring Fut8 expression compared with the LPA group in the scratch assay (Fig. 2G). The results of the transwell assay in peritoneal macrophages were consistent with those in RAW 264.7 cells(Supplementary Fig. 2C). Together with the previous data, these results supplied evidence that dysfunction of Fut8 has a direct relationship with the migration capacity of foam cells induced by LPA.

3.3. Regression of atherosclerosis plaques was accompanied by increased expression of Fut8

To gain insight into the functional role of Fut8 in atherosclerosis, we performed experiments *in vivo*. TC levels were notably high in the control group (nearly 10 mmol/L; normal-2.07 mmol/L [22]), whereas the rosuvastatin-treated group had lower TC levels. Importantly, compared with the control group, the rosuvastatin-treated group showed reduced TG and LDL-C levels (Fig. 3A). To further confirm the regression stage of atherosclerosis plaques, the results of Oil-Red O staining revealed that the neutral lipid content (expected to be primarily cholesteryl esters) was also decreased in the rosuvastatin groups (Fig. 3B). Interestingly, the results of H&E staining of the aortic valve demonstrated that the intimal thickness was increased in the control group compared with that in the baseline group, and it was decreased in the rosuvastatin group (Fig. 3C). Via immunohistochemistry staining, we found that the $CD68^{+}$ cell (marker of macrophage) content was significantly reduced in the rosuvastatin-treated groups compared with the control group (Fig. 3D). Thus, rosuvastatin promoted the regression of atherosclerosis plaques *in vivo*. The expression of Fut8 was detected by immunohistochemical staining. Compared with that in the control group, the expression of Fut8 was upregulated in the rosuvastatin group (Fig. 3E). Together with the above results, we concluded from these observations that regression of atherosclerosis plaques was accompanied by increased expression of Fut8.

3.4. $LPA_{1,3}$ receptors were activated and involved in regulation of the promoter activity of Fut8

LPA induces various cellular responses by interacting with specific cell surface G protein-coupled receptors (GPCR) of the endothelial differentiation gene (Edg) subfamily [23]. To further confirm whether LPA-induced diminished migration of foam cells is mediated by receptors, we examined the LPA receptor expression in RAW 264.7 cells. The relative abundance of LPA_1 and LPA_3 receptors was upregulated (Fig. 4A). Additionally, we observed that LPA_1 expression was higher than LPA_3 expression, consistent with the finding of a previous study [24]. To explore the role of Fut8 in LPA-$LPA_{1,3}$ receptor-migration pathways, we examined changes in Fut8 after inhibiting the receptors. After pretreatment with 10 μM Ki16425 (a competitive, potent and reversible antagonist to LPA_1, LPA_2 and LPA_3) for 1 h, protein expression of Fut8 and α-1, 6 fucosylation levels showed a significant increase compared with those in the LPA-treated group (Fig. 4B). Based on the above results, we found that protein and mRNA levels were downregulated in the LPA-treated group. To explore the reason why LPA decreased Fut8 protein levels, we asked whether LPA decreased Fut8 protein stability. We pretreated cells with cycloheximide (CHX) to inhibit protein translation [25]. The combination of CHX and LPA did not change Fut8 protein levels (Fig. 4C, Lane 4) compared with those for CHX treatment only (Fig. 4C, Lane 3), suggesting that the LPA-mediated decrease in Fut8 protein expression was not due to decreased stability of the protein but the process of synthesis. We also asked whether decreased Fut8 mRNA levels after LPA treatment were due to degraded Fut8 mRNA. Actinomycin D (AMD) was used to test Fut8 mRNA stability. The combination of AMD and LPA did not decrease Fut8 mRNA level compared with that for AMD treatment only (Fig. 4D) and even showed an increasing trend. These results demonstrated that LPA could affect the transcriptional level of Fut8 and did not degrade it. To explore the mechanism of decreased transcriptional levels, we tested the promoter activity of Fut8. The reporter gene pGL3-basic (which harbors the promoter region (−2095/-7) of mouse Fut8) was applied, luciferase activity analysis was conducted, and luciferase activity was measured to estimate promoter activity. As shown in Fig. 4E, luciferase activity was decreased significantly in the LPA-treated group in HEK293T cells. To demonstrate the most important functional region in the Fut8 promoter, HEK293T cells were cotransfected with a series of deletion constructs spanning the upstream region of the mouse *Fut8* gene. A deletion from −611 to −431 bp showed an apparent reverse of *Fut8* promoter activity (Fig. 4F), suggesting that certain elements required for *Fut8* promoter activity lie in the region between −611 and −431 bp.

3.5. HNF1α positively modulated the promoter activity of Fut8

By performing the first genome-wide association study (GWAS) of protein glycosylation, Lauc et al. found that HNF1α and its downstream target HNF4α regulated the expression of key fucosyltransferase and fucose biosynthesis genes. This finding revealed a new role for HNF1α as a master transcriptional regulator of multiple stages in the fucosylation process [26]. To explore the role of HNF1α in the regulation of Fut8, we first examined the change in expression of HNF1α. Whole-cell lysate was obtained, and the results of Western blotting showed that protein expression of HNF1α was decreased in the LPA-treated group

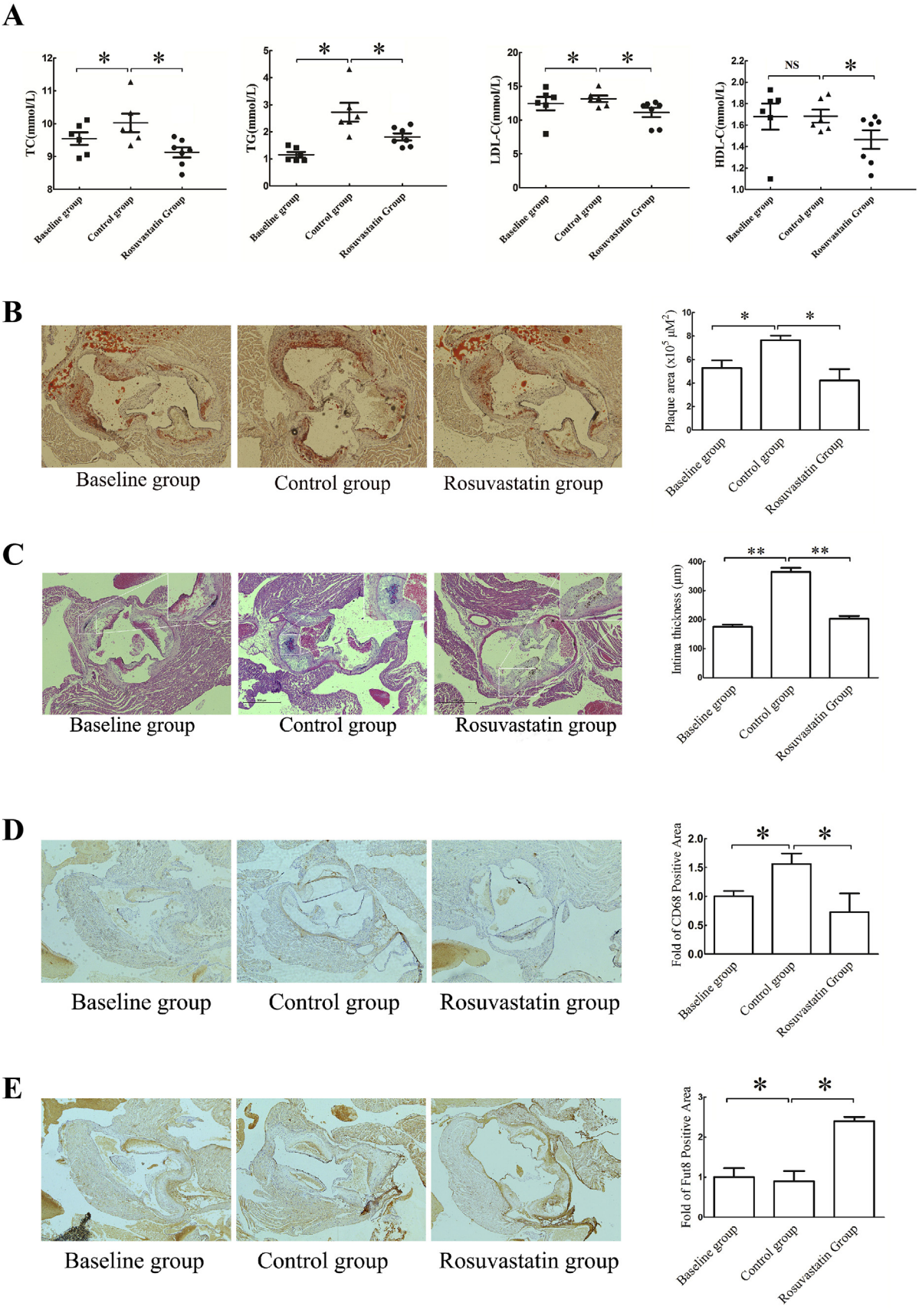

(caption on next page)

Fig. 3. Expression of Fut8 was restored in atherosclerosis regression *in vivo*.
(A) Serum TC, TG, LDL-C, HDL-C levels in three groups analyzed with an automatic analyzer. (B) Representative Oil-Red O stained images of whole aorta face and aortic sections (40X magnification). (C) Sectioned aorta sinus plaques stained with H&E (40X magnification). (D) Contents of macrophages ($CD68^+$) determined by immunohistochemistry staining in aorta sinus plaques (40X magnification). (E) Expression of Fut8 in aorta sinus plaques determined by immunohistochemistry staining (40X magnification). $^*p < 0.05$; $^{**}p < 0.01$. TC, total cholesterol; TG, triglyceride; LDL-C, low-density lipoprotein cholesterol; HDL-C, high-density lipoprotein cholesterol. (For interpretation of the references to colour in this figure legend, the reader is referred to the Web version of this article.)

(Fig. 5A). Immunofluorescence analysis revealed similar trends (Fig. 5B). Cytoplasmic protein levels of HNF1α were decreased (Fig. 5C), and nuclear protein levels of HNF1α showed more obvious decreasing trends in the LPA-treated group (Fig. 5D). To define the direct relationship between HNF1α and Fut8 expression, EMSA was performed using the biotin-labeled oligonucleotide probe containing the HNF1α binding sequence in the *Fut8* promoter to study the interactions between HNF1α and *Fut8* promoter. The results showed that LPA significantly decreased the DNA binding activity of HNF1α (Fig. 5E). To further confirm the direct binding of HNF1α and *Fut8* promoter, the ChIP assay was performed. HNF1α was immunoprecipitated with chromatin fragments prepared from RAW 264.7 cells in the presence or absence of LPA. The results demonstrated that the association of HNF1α with *Fut8* promoter was significantly decreased in LPA-treated cells (Fig. 5F). These results indicated that LPA decreased the binding of HNF1α with the *Fut8* promoter. Overexpression of HNF1α was facilitated by the pReceiver-M29 expression clone. The results in Fig. 5G demonstrated the effectiveness of the overexpression. The protein expression of Fut8 had reverse effects on the overexpression group compared with that for LPA only (Fig. 5H). Finally, we found that the numbers of migrated cells on the underside were much greater than those in the LPA group after overexpression of HNF1α in RAW 264.7 cells (Fig. 5I). Taken together, these results demonstrated that HNF1α had a positive effect on *Fut8* promoter region, and this effect was weakened after treatment with LPA. However, considering the result of Fig. 5I, we speculated that other factors might be working together with HNF1α.

4. Discussion

LPA is a structurally simple lipid phosphate ester with variability of the fatty acid chain length, saturation, and type of linkage to the glycerol backbone, thus affecting its biological functions [27]. Previous research has demonstrated that LPA was a key regulator of chemotaxis in different cell types [28]. In our experiments, LPA was used to stimulate the transformation from macrophages to foam cells, and high concentrations of serum in the lower chamber were used to alter the chemotactic capacity for foam cells. In another study, LPA was added to the lower chamber in the transwell assay to observe the effect of LPA on cell mobility. Indeed, we observed diminished mobility of foam cells induced by LPA, not the effect of LPA on cell mobility. Furthermore, different disease type, degree of saturation and function of concentration and time are also responsible for the multiple roles of LPA in biological activities. First, LPA has an opposite effect on cell mobility in different disease or cells. In human lung-resident mesenchymal stem cells, LPA activated the β-catenin pathway, which led to an increase of the migration capacity [29]. However, in the progression of atherosclerosis, high concentrations of LPA impair the capacity of monocyte-derived cells to migrate from the vessel wall, supporting a notion that LPA favors monocyte retention and foam cell formation in the subendothelium [5]. Our study simulated foam cell formation *in vitro*, and the results revealed that migration of foam cells induced by LPA was impaired. Second, several LPA subspecies can be found that vary based on the type of fatty acyl chain and linkage to the glycerol backbone, characteristics that affect biological activity [30]. In contrast to LPA18:0, Zhou et al. found that adherent monocytes directly start to migrate across the endothelium only in the LPA 20:4-treated arteries [31]. To evaluate whether other lipids could mimic PA action on human monocytes, a number of different phospholipids and their corresponding lyso-derivatives were tested in the chemotaxis assay. LysoPAs (18:1-lysoPA and 16:0-lysoPA) stimulated monocyte migration. From a quantitative point of view, lyso-PAs were similar to (16:0-LysoPA) or weaker (18:1-LysoPA) than the corresponding molecular species of PA [32]. The term LPA is used in our study to refer to the 18:1 species (unsaturated), which is also commonly used as a research reagent [33]. Third, LPA is reportedly able to stimulate cell proliferation of THP-1 monocytes at concentrations of 1 μM but not at higher concentrations (10 μM and 20 μM), despite induction of the expression of LPA receptors at the cellular level [34]. Gustin et al. clearly showed that LPA directly modulates monocyte chemotaxis, exerting the opposite effects according to its concentration. LPA was able to enhance monocyte migration at concentrations < 1 μM and inhibit their migration at LPA concentrations > 1 μM, as demonstrated using a chemotaxis assay. No effect was observed at 1 μM LPA. At higher LPA concentration (25 μM), the chemotactic response varies as a function of time. After 4 h, the chemotactic effect of the cytokines secreted by the EC is counteracted by the direct inhibitory effect of LPA on monocytes. For longer periods of time (24 h), monocyte migration was observed, likely due to lowered concentrations of bioactive LPA [35]. At low concentrations, LPA stimulates Rho, Rho-kinase, and myosin light chain phosphorylation, resulting in platelet shape changes caused by changes in the actin cytoskeleton [36]. At high concentrations, LPA stimulates Ca^{2+} mobilization and the tyrosine kinases Syk and Src, resulting in integrin $\alpha_{IIb}\beta3$ activation and aggregation [37]. Thus, 200 μM LPA used in this article represents a high concentration that simulated pathological conditions, and we observed the inhibition of foam cell migration. In reviewing the literature, the absolute concentration of circulating LPA in serum is detectable, ranging from 1 μM to 20 μM, across a number of pathological conditions [35,38]. However, LPA accumulated during atherogenesis induced by perivascular collar placement in *ApoE*$^{-/-}$ mice [39] and increased 13-fold in atheromatous plaques compared with that in normal arterial tissue [17]. Based on previous research, we speculated that a high concentration of LPA accumulated in the subendothelium, subsequently inducing the formation of foam cells and impairing the capacity of foam cell to migrate, leading to the build-up of necrotic pools under pathological conditions.

Previous research has demonstrated that glycosyltransferases have an impact on atherosclerosis. Homeister et al. found that Fut7-mediated α-1, 3/4 fucosylation of selectin ligands is necessary for P-selectin-dependent peripheral blood monocyte adhesion under shear stress [40]. ST3Gal-IV deficiency hindered the formation of the sugar-chain structure sLeX of CCR5 and subsequently impaired CCL5-triggered leukocyte arrest (known as firm adhesion) and recruitment under inflammatory conditions [41]. Our previous work found that degradation of ST6Gal-1 was the reason for the impairment of endothelial tight junctions by TNFα [10]. Based on the above studies, we concluded that the glycoprotein character of many important cell adhesion molecules, such as CCR5, P-selectin and VE-cadherin, might be responsible for the effects of glycosyltransferases on the processes of monocyte and endothelial cell adhesion and infiltration (earlier stages of atherosclerosis). As a modification enzyme, Fut8 cannot directly influence the migration of foam cells. For the moment, the target protein, which is related to cellular motor capacity and modified by Fut8, contains integrin α3β1 [42], TGF-β1 [43] and Unc-5 Netrin Receptor B (Unc5b). Via mass spectrum analysis and other experiments, we have demonstrated that Unc5b is related to cell mobility [44]. However, the relationship

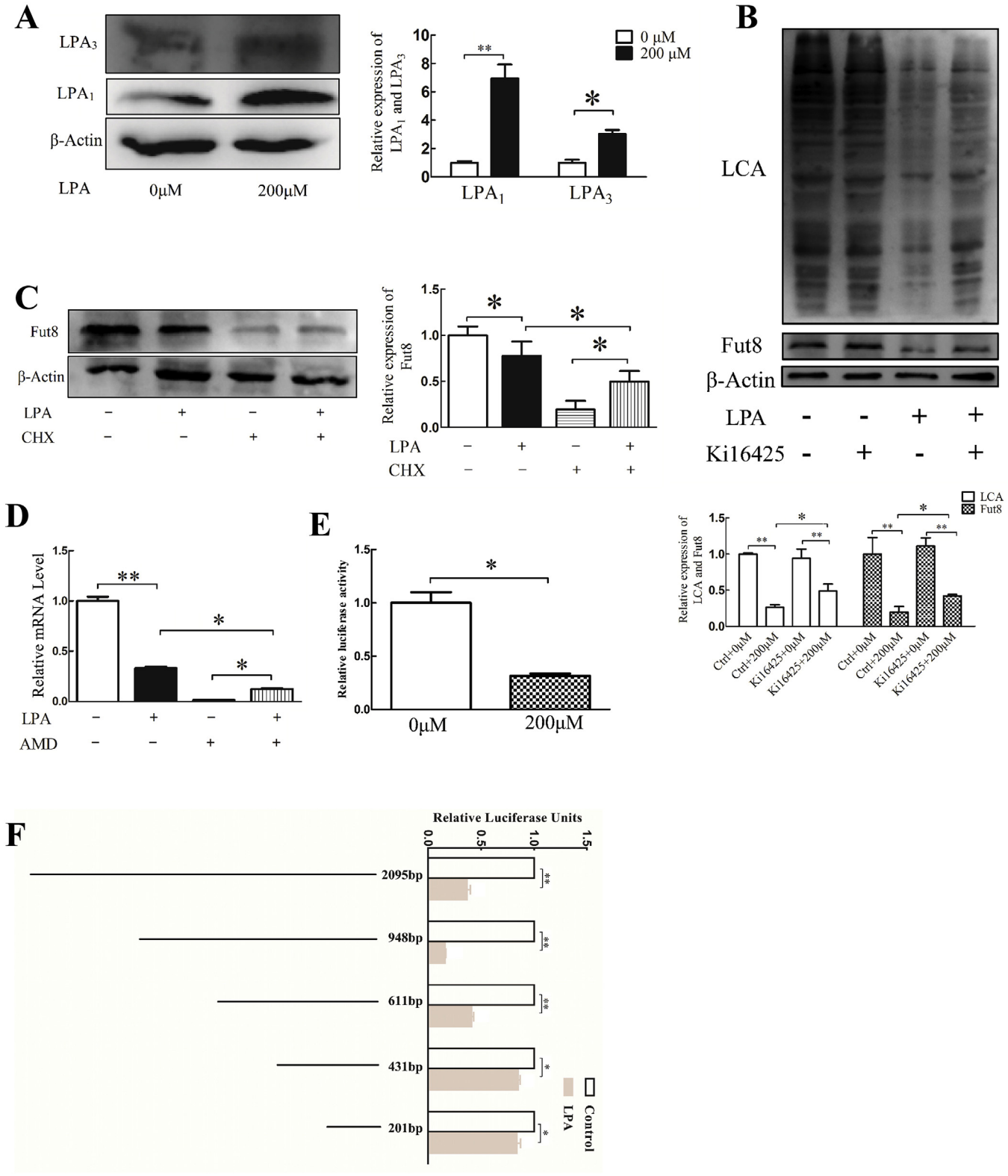

Fig. 4. $LPA_{1,\ 3}$ receptors were activated and involved in the regulation of the promoter activity of Fut8.
(A) Expression of LPA_1 and LPA_3 receptors detected by Western blot. (B) Pretreatment with 10 μM Ki16425 for 1 h; protein expression of Fut8 and α-1, 6 fucosylation detected by Western blot and lectin-blot. (C) Pretreatment with 10 μM CHX for 1 h; RAW 264.7 cells were treated with or without 200 μM LPA for 24 h. Total protein was isolated; immunoblot was performed using antibodies against Fut8 and actin. (D) RAW 264.7 cells were pretreated with 10 μM AMD (1 h) with or without 200 μM LPA for 24 h. Total mRNA was isolated; RT-PCR was performed using specific primers against *Fut8* and *actin*. (E) Luciferase activity measured according to the manufacturer's instructions. (F) pGL3-basic plasmids, containing a series of deletion constructs spanning the upstream region of the mouse *Fut8* gene, were transfected into HEK293T cells. Luciferase activity was measured according to the manufacturer's instructions. *$p < 0.05$; **$p < 0.01$. LPA, lysophosphatidic acid; CHX, Cycloheximide; AMD, actinomycin D.

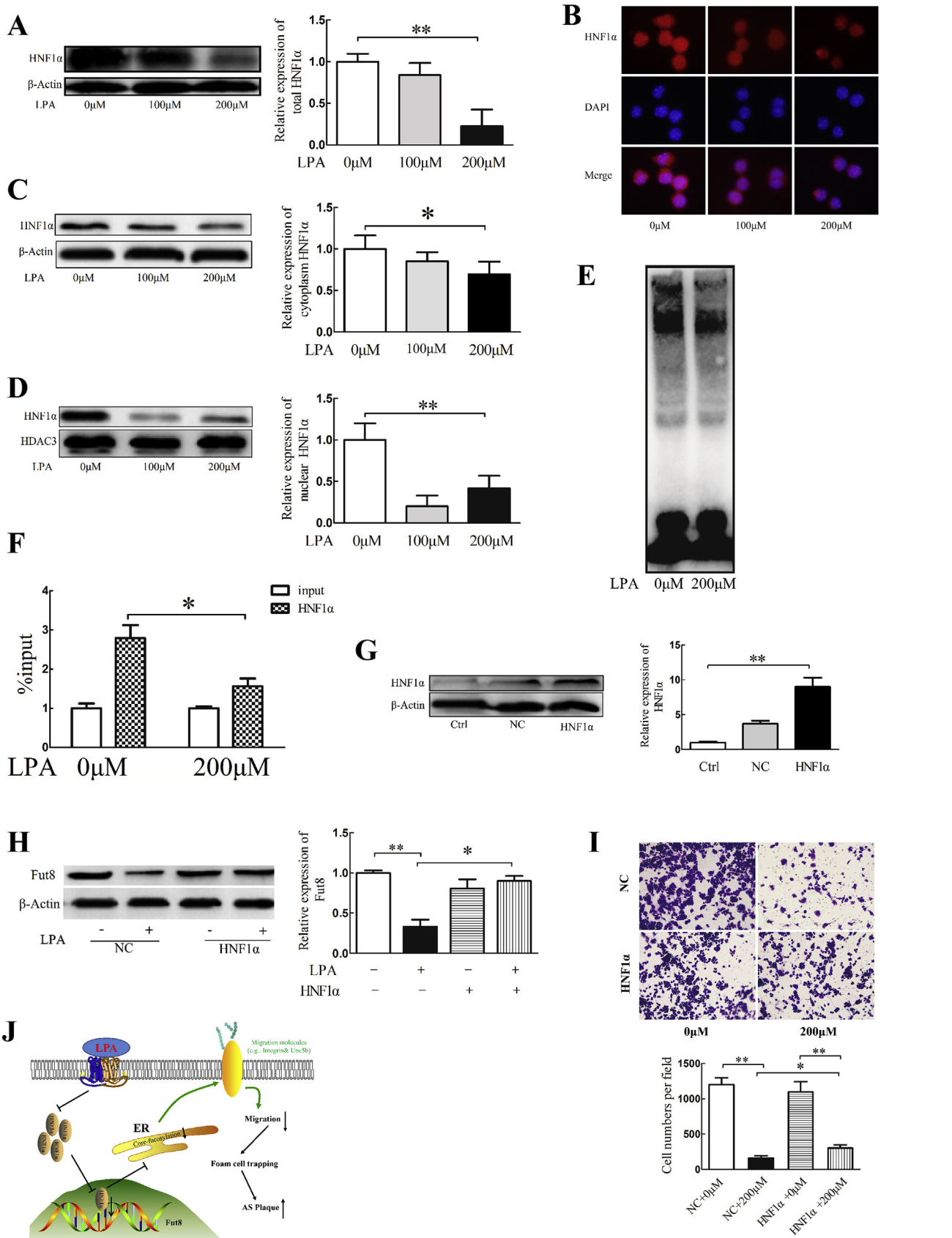

(caption on next page)

Fig. 5. Effect of HNF1α on regulation of Fut8 expression.
(A) Expression of HNF1α in whole-cell lysate detected by Western blot. (B) Fluorescence intensity of HNF1α was detected (1000X magnification). (C and D) Cytoplasmic and nuclear proteins were extracted using a nuclear and cytoplasmic protein extraction kit. Expression of HNF1α in the cytoplasm and nucleus was detected by Western blot. (E) EMSA was conducted to examine the DNA binding activity of HNF1α. The probe contained the potential HNF1α binding site located at −611/−431. (F) Chromatin from RAW 264.7 cells was immunoprecipitated with anti-HNF1α; the total extracted DNA set the input prior to immunoprecipitation, and the immunoprecipitated samples were PCR amplified using primers specific to a region that included the binding site, which is the specific binding site of HNF1α to the *Fut8* promoter. (G) The pReceiver-M29 Expression Clone was transfected into the RAW 264.7 cells. The effectiveness of overexpression was detected by Western blot. (H) Pretreatment with pReceiver-M29 expression clone for 24 h; protein and mRNA expression of Fut8 was evaluated by Western blot and RT-PCR. (I) Pretreatment with HNF1α plasmid for 24 h and 200 μM LPA for 24 h was used to induce foam cell formation. Migration of foam cells derived from RAW 264.7 cells was examined by transwell assay (400X magnification). (J) Model depicting Fut8-dependent mechanism of foam cell trapping in the plaque. $^{*}p < 0.05$; $^{**}p < 0.01$. LPA, lysophosphatidic acid; HNF1α, hepatocyte nuclear factor 1-alpha; HDAC3, Histone deacetylase 3; Ctrl, control; NC, negative control; ER, endoplasmic reticulum; AS, atherosclerosis.

between α-1, 6 fucosylation and Unc5b has not been explained. We are currently conducting follow-up experiments, and our next article will focus on the effect of α-1, 6 fucosylation modification of Unc5b on cell movement.

In this investigation, it was found that α-1, 6 fucosylation was downregulated in foam cells. Knockdown of *Fut8* gene resulted in downregulation of the migration of foam cells, and restoration of Fut8 expression increased the migration of foam cells. Although we observed changes in the expression of Fut7, α-1, 3/4 fucosylation showed no significant changes. We speculated that Fut7 enzymatic activity might be greater than that of Fut8, thus compensating for the downregulation of Fut7. We concluded that decreased Fut8 expression had a direct relationship with the diminished capacity of foam cell migration.

HNF1α, which is the most important transactivator in liver-specific gene expression, binds to similar regulatory cis elements such as albumin, β-fibrinogen and α1-antitrypsin genes [45]. Limited work has been performed to explore the regulator role of HNF1α in Fut8. By conducting the first genome-wide association study (GWAS) of protein glycosylation, Lauc et al. found that HNF1α enhanced the activity of antennary Futs (Fut3, Fut5, etc.) and increased the amount of GDP-fucose available for antennary fucosylation by suppressing Fut8, which adds fucose to the core-GlcNAc [26]. We observed differences between the results. Indeed, knockdown of HNF1α had the opposite effects on Fut8 expression in HepG2 or Panc1 cell lines in this study. In addition, in the ChIP experiments, a limited number of sites were identified in the regulatory regions of Fut3, Fut5, Fut6, and Fut10, and any HNF binding sequences within the Fut8 regulatory elements could not be detected. However, Odom et al. noted that the sites are not conserved between primates and rodents [46]. Another report found that the large family of genes that add fucose to proteins and lipids (Fucosyltransferases, Futs) had a highly complex evolutionary history, including several more recent events specific to primates [47]. The results of this study indicated that HNF1α had a positive effect on the *Fut8* promoter region and that it was weakened after treatment with LPA. However, HNF1α usually participates in the regulation in the form of complex molecules. For example, HNF1α protein, CBP protein, P/CAF protein, Src-1 protein and RAC 3 protein formed a chromosomal recombination complex [48]. P300 acts as a cofactor with HNF1α to coordinate the transcription of the glucose metabolism gene *GLUT2* [49]. Our team also found that FOX3a, SRBP2 and HNF1α play a role in the expression of certain genes in the liver such as *LDLR* [50]. However, our study did not detect expression of HNF4α. Therefore, the mechanism of regulation of Fut8 by HNF1α may be different from that proposed in Lauc et al.'s study, and the detailed mechanism requires additional research.

In summary, our research revealed that Fut8 and α-1, 6 fucosylation were downregulated in the process of foam cell formation and these changes were directly associated with the diminished mobility of foam cells, which might be responsible for the lipid deposits in the endometrium. $LPA_{1,\ 3}$ receptor and HNF1α were found to play important roles in the downregulation of Fut8. This study offered novel insights into glycosyltransferases in foam cell retention and suggested that promoting Fut8 expression could represent a new approach for treating atherosclerosis.

Conflicts of interest

The authors declared they do not have anything to disclose regarding conflict of interest with respect to this manuscript.

Financial support

This work was supported by the National Natural Science Foundation of China, China (No. 81370403), the Chongqing Foundation and Advanced Research Project (No. CSTC2015jcyjBX0053), the Chongqing Medical University Scientific Research Cultivating Fund (No. 201414), and the Natural Science Foundation of the Chongqing Science and Technology Committee (No. cstc2015jcyjA10002).

Author contributions

L. Chen and C. Yu designed the research; L. Chen and X. Yang performed the *in vitro* research; L. Chen, X. Deng and Y. Liu performed the *in vivo* research; and J. Zhang performed the double luciferase assay. L. Chen and J. Zhang analyzed the data, and L. Chen wrote and edited the paper. All authors reviewed and approved the manuscript.

Acknowledgments

The authors thank Yanlei Guo for assistance with animal experiments.

Appendix A. Supplementary data

Supplementary data to this article can be found online at https://doi.org/10.1016/j.atherosclerosis.2019.09.001.

References

[1] M. Writing Group, D. Mozaffarian, E.J. Benjamin, et al., Heart disease and stroke statistics-2016 update: a report from the American heart association, Circulation 133 (2016) e38–360.
[2] C.K. Glass, J.L. Witztum, Atherosclerosis. the road ahead, Cell 104 (2001) 503–516.
[3] Y.M. Park, M. Febbraio, R.L. Silverstein, CD36 modulates migration of mouse and human macrophages in response to oxidized LDL and may contribute to macrophage trapping in the arterial intima, J. Clin. Investig. 119 (2009) 136–145.
[4] K.J. Moore, F.J. Sheedy, E.A. Fisher, Macrophages in atherosclerosis: a dynamic balance, Nat. Rev. Immunol. 13 (2013) 709–721.
[5] J. Llodra, V. Angeli, J. Liu, et al., Emigration of monocyte-derived cells from atherosclerotic lesions characterizes regressive, but not progressive, plaques, Proc. Natl. Acad. Sci. U.S.A. 101 (2004) 11779–11784.
[6] J.E. Feig, J.X. Rong, R. Shamir, et al., HDL promotes rapid atherosclerosis regression in mice and alters inflammatory properties of plaque monocyte-derived cells, Proc. Natl. Acad. Sci. U.S.A. 108 (2011) 7166–7171.
[7] J. Schoberer, Y.J. Shin, U. Vavra, et al., Analysis of protein glycosylation in the ER, Methods Mol. Biol. 1691 (2018) 205–222.
[8] R.A. Dwek, Glycobiology: more functions for oligosaccharides, Science 269 (1995) 1234–1235.
[9] Y. Doring, H. Noels, M. Mandl, et al., Deficiency of the sialyltransferase St3Gal4 reduces Ccl5-mediated myeloid cell recruitment and arrest: short communication, Circ. Res. 114 (2014) 976–981.
[10] X. Deng, J. Zhang, Y. Liu, et al., TNF-alpha regulates the proteolytic degradation of

ST6Gal-1 and endothelial cell-cell junctions through upregulating expression of BACE1, Sci. Rep. 7 (2017) 40256.
[11] J. Zhang, Y. Liu, X. Deng, et al., ST6GAL1 negatively regulates monocyte transendothelial migration and atherosclerosis development, Biochem. Biophys. Res. Commun. 500 (2018) 249–255.
[12] X. Wang, J. Chen, Q.K. Li, et al., Overexpression of alpha (1,6) fucosyltransferase associated with aggressive prostate cancer, Glycobiology 24 (2014) 935–944.
[13] K. Shao, Z.Y. Chen, S. Gautam, et al., Posttranslational modification of E-cadherin by core fucosylation regulates Src activation and induces epithelial-mesenchymal transition-like process in lung cancer cells, Glycobiology 26 (2016) 142–154.
[14] Y.P. Zhao, X.Y. Xu, M. Fang, et al., Decreased core-fucosylation contributes to malignancy in gastric cancer, PLoS One 9 (2014) e94536.
[15] L. Chen, J. Zhang, X. Deng, et al., Lysophosphatidic acid directly induces macrophage-derived foam cell formation by blocking the expression of SRBI, Biochem. Biophys. Res. Commun. 491 (2017) 587–594.
[16] H. Zhao, T. Han, X. Hong, et al., Adipose differentiationrelated protein knockdown inhibits vascular smooth muscle cell proliferation and migration and attenuates neointima formation, Mol. Med. Rep. 16 (2017) 3079–3086.
[17] W. Siess, K.J. Zangl, M. Essler, et al., Lysophosphatidic acid mediates the rapid activation of platelets and endothelial cells by mildly oxidized low density lipoprotein and accumulates in human atherosclerotic lesions, Proc. Natl. Acad. Sci. U. S. A. 96 (1999) 6931–6936.
[18] M.Z. Cui, Lysophosphatidic acid effects on atherosclerosis and thrombosis, Clin. Lipidol. 6 (2011) 413–426.
[19] Q. Pu, C. Yu, Glycosyltransferases, glycosylation and atherosclerosis, Glycoconj. J. 31 (2014) 605–611.
[20] J. Lis-Kuberka, I. Katnik-Prastowska, M. Berghausen-Mazur, et al., Lectin-based analysis of fucosylated glycoproteins of human skim milk during 47 days of lactation, Glycoconj. J. 32 (2015) 665–674.
[21] D.J. Becker, J.B. Lowe, Fucose: biosynthesis and biological function in mammals, Glycobiology 13 (2003) 41R–53R.
[22] S.H. Zhang, R.L. Reddick, J.A. Piedrahita, et al., Spontaneous hypercholesterolemia and arterial lesions in mice lacking apolipoprotein E, Science 258 (1992) 468–471.
[23] E.J. Goetzl, S. An, Diversity of cellular receptors and functions for the lysophospholipid growth factors lysophosphatidic acid and sphingosine 1-phosphate, FASEB J. : Off. Publ. Feder. Am. Soc. Exp. Biol. 12 (1998) 1589–1598.
[24] P. Subramanian, E. Karshovska, P. Reinhard, et al., Lysophosphatidic acid receptors LPA1 and LPA3 promote CXCL12-mediated smooth muscle progenitor cell recruitment in neointima formation, Circ. Res. 107 (2010) 96–105.
[25] T.G. Obrig, W.J. Culp, W.L. McKeehan, et al., The mechanism by which cycloheximide and related glutarimide antibiotics inhibit peptide synthesis on reticulocyte ribosomes, J. Biol. Chem. 246 (1971) 174–181.
[26] G. Lauc, A. Essafi, J.E. Huffman, et al., Genomics meets glycomics-the first GWAS study of human N-Glycome identifies HNF1alpha as a master regulator of plasma protein fucosylation, PLoS Genet. 6 (2010) e1001256.
[27] G.B. Mills, W.H. Moolenaar, The emerging role of lysophosphatidic acid in cancer, Nat. Rev. Cancer 3 (2003) 582–591.
[28] S. Willier, E. Butt, T.G. Grunewald, Lysophosphatidic acid (LPA) signalling in cell migration and cancer invasion: a focussed review and analysis of LPA receptor gene expression on the basis of more than 1700 cancer microarrays, Biol. Cell 105 (2013) 317–333.
[29] L. Badri, V.N. Lama, Lysophosphatidic acid induces migration of human lung-resident mesenchymal stem cells through the beta-catenin pathway, Stem Cells 30 (2012) 2010–2019.
[30] J. Aoki, A. Inoue, S. Okudaira, Two pathways for lysophosphatidic acid production, Biochim. Biophys. Acta 1781 (2008) 513–518.
[31] Z. Zhou, P. Subramanian, G. Sevilmis, et al., Lipoprotein-derived lysophosphatidic acid promotes atherosclerosis by releasing CXCL1 from the endothelium, Cell Metabol. 13 (2011) 592–600.
[32] D. Zhou, W. Luini, S. Bernasconi, et al., Phosphatidic acid and lysophosphatidic acid induce haptotactic migration of human monocytes, J. Biol. Chem. 270 (1995) 25549–25556.
[33] Y.C. Yung, N.C. Stoddard, J. Chun, LPA receptor signaling: pharmacology, physiology, and pathophysiology, J. Lipid Res. 55 (2014) 1192–1214.
[34] F. D'Aquilio, M. Procaccini, V. Izzi, et al., Activatory properties of lysophosphatidic acid on human THP-1 cells, Inflammation 30 (2007) 167–177.
[35] C. Gustin, M. Van Steenbrugge, M. Raes, LPA modulates monocyte migration directly and via LPA-stimulated endothelial cells, Am. J. Physiol. Cell Physiol. 295 (2008) C905–C914.
[36] M. Retzer, M. Essler, Lysophosphatidic acid-induced platelet shape change proceeds via Rho/Rho kinase-mediated myosin light-chain and moesin phosphorylation, Cell. Signal. 12 (2000) 645–648.
[37] P. Maschberger, M. Bauer, J. Baumann-Siemons, et al., Mildly oxidized low density lipoprotein rapidly stimulates via activation of the lysophosphatidic acid receptor Src family and Syk tyrosine kinases and Ca2+ influx in human platelets, J. Biol. Chem. 275 (2000) 19159–19166.
[38] M.E. Lin, D.R. Herr, J. Chun, Lysophosphatidic acid (LPA) receptors: signaling properties and disease relevance, Prostaglandins Other Lipid Mediat. 91 (2010) 130–138.
[39] M. Bot, I. Bot, R. Lopez-Vales, et al., Atherosclerotic lesion progression changes lysophosphatidic acid homeostasis to favor its accumulation, Am. J. Pathol. 176 (2010) 3073–3084.
[40] J.W. Homeister, A. Daugherty, J.B. Lowe, Alpha(1,3)fucosyltransferases FucT-IV and FucT-VII control susceptibility to atherosclerosis in apolipoprotein E-/- mice, Arterioscler. Thromb. Vasc. Biol. 24 (2004) 1897–1903.
[41] M. Sperandio, D. Frommhold, I. Babushkina, et al., Alpha 2,3-sialyltransferase-IV is essential for L-selectin ligand function in inflammation, Eur. J. Immunol. 36 (2006) 3207–3215.
[42] Y. Zhao, S. Itoh, X. Wang, et al., Deletion of core fucosylation on alpha3beta1 integrin down-regulates its functions, J. Biol. Chem. 281 (2006) 38343–38350.
[43] X. Wang, S. Inoue, J. Gu, et al., Dysregulation of TGF-beta1 receptor activation leads to abnormal lung development and emphysema-like phenotype in core fucose-deficient mice, Proc. Natl. Acad. Sci. U.S.A. 102 (2005) 15791–15796.
[44] X. Yang, J. Zhang, L. Chen, et al., The role of UNC5b in ox-LDL inhibiting migration of RAW264.7 macrophages and the involvement of CCR7, Biochem. Biophys. Res. Commun. 505 (2018) 637–643.
[45] H. Schrem, J. Klempnauer, J. Borlak, Liver-enriched transcription factors in liver function and development. Part II: the C/EBPs and D site-binding protein in cell cycle control, carcinogenesis, circadian gene regulation, liver regeneration, apoptosis, and liver-specific gene regulation, Pharmacol. Rev. 56 (2004) 291–330.
[46] D.T. Odom, R.D. Dowell, E.S. Jacobsen, et al., Tissue-specific transcriptional regulation has diverged significantly between human and mouse, Nat. Genet. 39 (2007) 730–732.
[47] C. Javaud, F. Dupuy, A. Maftah, et al., The fucosyltransferase gene family: an amazing summary of the underlying mechanisms of gene evolution, Genetica 118 (2003) 157–170.
[48] L. Waters, B. Yue, V. Veverka, et al., Structural diversity in p160/CREB-binding protein coactivator complexes, J. Biol. Chem. 281 (2006) 14787–14795.
[49] N. Ban, Y. Yamada, Y. Someya, et al., Hepatocyte nuclear factor-1alpha recruits the transcriptional co-activator p300 on the GLUT2 gene promoter, Diabetes 51 (2002) 1409–1418.
[50] X. Yang, J. Zhang, L. Chen, et al., Chitosan oligosaccharides enhance lipid droplets via down-regulation of PCSK9 gene expression in HepG2 cells, Exp. Cell Res. 366 (2018) 152–160.